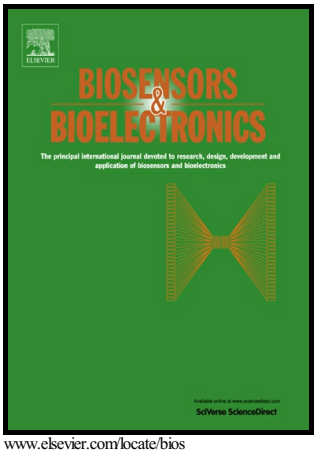

www.elsevier.com/locate/bios

In situ grown DNA nanotail-templated silver nanoclusters enabling label-free electrochemical sensing of terminal deoxynucleotidyl transferase activity

Yufang Hu, Qingqing Zhang, Zhiyong Guo, Sui Wang, Chunnuan Du, Chunyang Zhai

PII: S0956-5663(17)30391-3
DOI: http://dx.doi.org/10.1016/j.bios.2017.06.017
Reference: BIOS9787

To appear in: *Biosensors and Bioelectronic*

Received date: 4 March 2017
Revised date: 6 June 2017
Accepted date: 8 June 2017

Cite this article as: Yufang Hu, Qingqing Zhang, Zhiyong Guo, Sui Wang, Chunnuan Du and Chunyang Zhai, *In situ* grown DNA nanotail-templated silve nanoclusters enabling label-free electrochemical sensing of termina deoxynucleotidyl transferase activity, *Biosensors and Bioelectronic* http://dx.doi.org/10.1016/j.bios.2017.06.017

In situ grown DNA nanotail-templated silver nanoclusters enabling label-free electrochemical sensing of terminal deoxynucleotidyl transferase activity

Yufang Hu*, Qingqing Zhang, Zhiyong Guo, Sui Wang, Chunnuan Du, Chunyang Zhai

Faculty of Materials Science and Chemical Engineering, Ningbo University, Ningbo, 315211, P. R. China

*To whom correspondence should be addressed. Phone: +86-574-87600798. Fax: +86-574-87600798. E-mail: huyufang@nbu.edu.cn.

Abstract

A novel label-free electrochemical strategy was established based on the unique electro-catalytic activity of graphene oxide (GO)-supported terminal deoxynucleotidyl transferase (TdT)-generated C-rich DNA nanotail-templated silver nanoclusters (DNA-AgNCs). TdT can catalyze the deoxycytidine triphosphate (dCTP) to the 3'-OH terminus of single-stranded DNA (ssDNA) with no template; then, in the presence of Ag(I), TdT-generated C-rich DNA sequence was employed for the synthetic template of AgNCs because of the formed complexes of nitrogen atoms of cytosine based with silver atoms. We proved that *in situ* grown DNA nanotail-templated AgNCs can be adsorbed on GO-modified electrode and possess high electro-catalytic activity to H_2O_2 reduction, presenting a good electrochemical indicator for signal readout. Under optimal conditions, the proposed biosensor could be employed for quantitatively monitoring TdT activity and within a dynamic range from 0.4 to 90 U/mL and a low limit of detection is 0.08 U/mL. With high sensitivity

and excellent selectivity, this strategy offers a facile, convenient and specific electrochemical method for TdT activity detection and its relevant inhibitors screening. It holds a promising potential in the practical application of TdT-based biochemical research, disease diagnosis and drug discovery.

Keywords: Terminal deoxynucleotidyl transferase; Silver nanoclusters; Graphene oxide; Enzyme activity; Inhibitor

1. Introduction

A common feature to all polymerases is to act in a template-dependent manner so that they require a DNA strand to direct the polymerization process (Gopalakrishnan et al., 2003). However, this mechanism differs for just one type of DNA polymerizing enzyme, called terminal deoxynucleotidyl transferase (TdT) (Bollum et al., 1964) which can directly catalyze the incorporation of multiple dNTP or small molecule conjugated dNTP into a single-strand DNA without needing a template strand. The preferred substrate for this enzyme are 3’ protruding ends, but it is also able to add nucleotides to blunt and 3’-recessed ends of double strand DNA fragments (Liu et al., 2016; Shen et al., 2015; Wang et al., 2016). TdT was one of the first DNA polymerases identified in mammalian cells (Bollum et al., 1960) first from thymus and later in bone marrow (Krayevsky et al., 2000). As recorded, TdT is overexpressed in some cancer types, where it might compete with pol μ during the mutagenic repair of double strand breaks through the nonhomologous end joining pathway (Benedict et

al., 2000; Benedict et al., 1999). Numerous clinical studies also showed that altered expression levels and activity of TdT have a critical role for cancer development and might worsen the response to anticancer chemotherapy (Greaves et al., 1980). TdT overexpression has been observed in B and T cell acute lymphocytic leukemia (ALL) and acute myelocitic leukemia (AML) (Hoffbrand et al., 1977; Kung et al., 1978). Generally, the TdT expression in AML patients is quite variable, whereas in ALL patients TdT is overexpressed in about 90% of cases, and this overexpression correlates to poor prognosis and response to chemotherapy (Venditti et al., 1997). Hence, probing the properties and functions of TdT enzymes is significant for cancer-related fundamental biochemical research and pharmaceutical development.

Traditionally, detection of TdT activity relies on biochemical assay, immunoassay, and gel electrophoresis (Goldschneider et al., 1977; Kung et al., 1976; Kung et al., 1978), which are hampered by some technical barriers including hazards of radioactive or fluorescent labeled DNA or nucleotides, and intricate multistep procedures which are time-consuming, expensive, and labor-intensive. Accordingly, the non-radioactive or label-free TdT assays attract increasing research interests. Most of currently available non-radioactive or label-free TdT assays are fluorescent methods, such as peroxidase-mimic DNAzyme-randomly arrayed G-rich sequence binding to thioflavin T (Liu et al., 2014), polyT-templated copper nanoparticles as promising fluorescent probe (Peng et al., 2015), and the synthesis of silver nanoclusters by long-chain cytosine-rich DNA (Yuan et al., 2014). Except the fluorescence technique, other analytical techniques are seldom implicated in TdT

assays, presenting a large unexplored field to investigate. As a promising handy detection technique, electrochemical biosensors have received increasing attention due to their intrinsic advantages of high sensitivity, good portability, simple instrumentation, low cost, and promising response speed (Labib et al., 2016; Mahshid et al., 2015). From this viewpoint electrochemical analysis of TdT activity has good perspectives in diseases diagnostics and drug discovery. However, the reported electrochemical biosensor for TdT activity detection is scarce. Hence, it is still challenging and highly desirable to develop new label-free electrochemical mechanism to monitor the activity of TdT.

Recent developments in metal nanoclusters (NCs) have received great attention because of their excellent properties of large surface area and good electronic properties, and also hold promise for several applications, including (but not limited to) catalysis (including fuel cell catalysts), photochemistry nanoelectronics chemical sensors and many others (Elghanian et al., 1997; Jin et al., 2016; Jin et al., 2016; Zhao et al., 2016), in which silver nanoclusters (AgNCs) is a typical representative. Currently, polynucleotide-templated silver nanoclusters, made up of a few silver atoms and are usually smaller than 2 nm in diameter, have been applied to different fields, such as chemical-sensing, in vitro bioassays and in vivo biological imaging (Javani et al., 2016; Liu et al., 2015; Wang et al., 2016). Additionally, it has been also reported that the electrochemical sensing can be realized by the catalytic activity of Ag atoms in AgNCs (Xia et al., 2013; Yang et al., 2015). Up to now, to the best of our knowledge, the application of TdT-derived AgNCs in electrochemical biosensing for

TdT activity detection remains largely unexplored.

In this work, we developed a novel electrochemical assay for label-free detection of TdT activity based on the unique electro-catalytic activity of the TdT-related DNA-AgNCs loaded on the graphene oxide (GO)-modified electrode. TdT, the exceptive polymerase of cancer related-disease, can catalyze the addition of deoxyribonucleoside triphosphates (dNTP) to the 3'-OH terminus of single-stranded DNA (ssDNA) with the length of three or more nucleotides. Herein, since massive deoxycytidine triphosphates (dCTP) are free, the potential TdT-yielded C-rich DNA nanotail-templated AgNCs (DNA-AgNCs) was generated by a random C-rich DNA sequence via TdT polymerization. The detection mechanism of the proposed TdT electrochemical sensor relied on three intriguing phenomena that we found: (1) ssDNA and dCTP by the extension of TdT are capable of *in situ* generation of a random C-rich DNA sequence, which can be used as the template for the formation of AgNCs due to the formed complexes of nitrogen atoms of cytosine based with silver atoms; (2) inspired by the strong and selective interaction of ssDNA, with two-dimensional carbon nanomaterials, such as GO (Feng et al., 2016; Hu et al., 2015; Singh et al., 2016; Zhang et al., 2017), we investigated the interaction of TdT-related DNA-AgNCs and GO and discovered that TdT-generated C-rich DNA can easily and effectively bind with GO through π-π stacking interaction; (3) we further demonstrated that TdT-related DNA-AgNCs adsorbed on GO-modified electrode possess high electro-catalytic activity to H_2O_2 reduction. Consequently, the quantitative detection of TdT activity was achieved via electrochemical measurement

of DNA-AgNCs generation. This electrochemical biosensor was highly sensitive and selective, and displays good feasibility for TdT inhibitor screening. The proposed strategy presents a novel method for TdT activity detection, which is helpful for further development of a miniaturized and low-cost electrochemical sensing platform for TdT-targeted biochemical investigation and drug discovery.

2. Experimental

2.1. Materials and Apparatus

Terminal deoxynucleotidyl transferase (TdT), single-stranded DNA (ssDNA) (5'-ATG GGC ATG AAC-3'), deoxycytidine triphosphate (dCTP) and reaction buffer for TdT (1 M potassium cacodylate, 0.125 M Tris, 0.05% (v/v) Triton X-100, 5 mM $CoCl_2$ (pH 7.2)) were obtained from Shanghai Sangon Biotechnology Co. Ltd. (Shanghai, China). H_2O_2 (30 wt%), $AgNO_3$, $NaBH_4$, $Na_4P_2O_7 \cdot 10H_2O$ (PP) were purchased from Sinopharm Chemical Reagent Co. Ltd (China). Graphite powder (99.99995%, 325 mesh) was purchased from Alfa Aesar. The preparation of graphene oxide (GO) was custom-synthesized by Hummer's method (William et al., 1958). Glucose (GLC), dopamine (DA), ascorbic acid (AA), citric acid (CA), papain, thrombin, lysozyme (LZM) and acetyl cholinesterase (AChE) were obtained from the Aladdin Industrial Corporation. All chemicals were of analytical grade without further purification. Excepting special statement, all electrochemical experiments were performed in PBS at room temperature. All solutions were prepared with double-distilled water (18.25 MΩ cm) from the Millipore Milli-Q system.

Electrochemical measurements were performed on a CHI 660E electrochemical workstation (Chenhua Instrument Company of Shanghai, China) and a conventional three-electrode system, which consisted of a glassy carbon working electrode (3 mm in diameter), a platinum foil counter electrode, and a saturated Ag/AgCl reference electrode. All the potentials used in this work were with respect to the Ag/AgCl reference electrode. Fluorescence spectra were measured at room temperature in a 100 μL quartz cuvette on a Hitachi F-4600 spectrometer (Hitachi Co. Ltd., Japan). Particle size analysis was acquired using a Malvern Zana ZS 90 Mastersizer. Polyacrylamide gel electrophoresis (PAGE) was scanned by a ChemiDoc™ MP System, Bio-Rad, USA.

2.2. Preparation of TdT-yielded DNA-AgNCs

The synthesized process of TdT-generated C-rich DNA nanotail-templated AgNCs is displayed in Scheme 1.

In situ TdT-generated C-rich DNA nanotail (noted as TdT-yielded DNA): The polymerization solution comprised TdT (20 U/μL, 0.1 μL), ssDNA (10 μM, 2.5 μL), dCTP (10 mM, 0.5 μL), reaction buffer for TdT (1 μL) and double-distilled water (0.9 μL). After incubation for 1 h at 37 °C in the water bath, the polymerization reaction was stopped by heating at 75 °C for 15 min to inactivate the enzyme. The polymerization mixture was subsequently used for the formation of DNA-AgNCs.

Grown DNA nanotail-templated AgNCs (namely DNA-AgNCs): $AgNO_3$ (1 mM, 5 μL), phosphate buffer (0.1 M, pH 7.0, 25 μL) and double-distilled water (10 μL) were added to the above polymerization mixture (5 μL). After incubation in an ice

bath for 15 min, the mixture was reduced by adding freshly prepared $NaBH_4$ aqueous solution (1 mM, 5 μL) under vigorous shaking. The shaking was kept for 2 min to make sure that silver ions were adequately reduced. The mixture was then kept in the dark for 1.5 h at room temperature. Afterward, the obtained DNA-AgNCs were stored at 4 °C in the dark when not in use. The excitation and emission spectra of DNA-AgNCs were recorded on the Hitachi F-4600 spectrometer.

2.3. Fabrication of the DNA-AgNCs/GO/GCE

GCE:

Prior to modification, glassy carbon electrode (GCE, 3 mm diameter) was polished on a microcloth with 1.0, 0.3, and 0.05 μm alumina slurry respectively and successively sonicated in double-distilled water, ethanol, and double-distilled water for 5 min, and then dried in air at room temperature.

GO/GCE:

The GO suspension (1.0 mg/mL) was obtained by ultrasonicating GO in HAc-NaAc buffer (0.1 M, pH 5.0) for 2 h. The GO-modified glassy carbon electrodes (GO/GCE) were prepared by electrodepositing GO onto the surface of bare GCE and the cyclic voltammetry potential was cyclically swept from -1.5 to +0.5 V at 10 mV/s under stirring for 5 cycles. Then, the as-prepared GO-modified electrodes were used for subsequent detection experiments.

DNA-AgNCs/GO/GCE:

5 μL of the grown DNA nanotail-templated AgNCs solution above was dropped onto the surface of GO/GCE to obtain DNA-AgNCs/GO/GCE. The prepared

electrode was rinsed completely with phosphate buffer (0.1 M, pH 7.0). After incubation for 15 min, the prepared DNA-AgNCs/GO/GCE was subjected to 50 mV/s cyclic voltammetry scans in phosphate buffer within the potential range from -1.2 to 0 V. The modified electrodes were stored at 4 °C in PBS (0.1 M, pH 7.0) when not in use.

2.4. Assay of terminal deoxynucleotidyl transferase (TdT) activity

For TdT activity analysis, TdT at various final concentrations (0, 0.4, 1.2, 1.6, 2, 2.4, 2.8, 3.2, 3.6, 4, 8, 12, 16, 20, 24, 28, 32, 36, 40, 50, 60, 70, 80, 90, 100 and 120 U/mL) was incubated with ssDNA (10 μM, 2.5 μL), dCTP (10 mM, 0.5 μL), reaction buffer for TdT (1 μL) and double-distilled water (0.9 μL) with a total volume of 5 μL. After that, the synthetized TdT-mediated C-rich DNA nanotails were employed as the template for the formation of AgNCs under $NaBH_4$ aqueous solution. The total reaction conditions were confirmed as described in Section 2.2. Ultimately, the prepared DNA-AgNCs were applied to further electrochemical measurements under the same conditions as those mentioned in Section 2.3.

2.5. Inhibition assay of TdT activity

TdT (20 U/μL, 0.1 μL) and sodium pyrophosphate (PP) at various final concentrations (0, 0.01, 0.02, 0.05, 0.1, 0.5, 1, 1.5, 2, 3, 4, 5, 6, 7 and 8 mM) were pre-incubated with ssDNA (10 μM, 2.5 μL), dCTP (10 mM, 0.5 μL), reaction buffer for TdT (1 μL) and double-distilled water (0.9 μL) with a total volume of 5 μL. Subsequently, the preparation of DNA-AgNCs and other reaction conditions were employed as described above.

3. Results and discussion

3.1. Principle and feasibility of the assay

Terminal deoxynucletidyl transferase (TdT) is overexpressed in some cancer types, where TdT activity has a critical role for cancer development and might worsen the response to anticancer chemotherapy. Hence, it would be of great interest to investigate the activity of TdT and screen its inhibitors. The key of our label-free electrochemical strategy for the TdT activity detection is the exploitation of TdT to generate C-rich DNA nanotails, which can be used as the template of the formation of DNA-AgNCs. As depicted in Scheme 1, in the presence of dCTP, TdT catalyzes the repetitive addition of deoxynucleotide to elongate the 3'-OH end of DNA primer, and the grown C-rich DNA nanotails were performed for the formation of DNA-AgNCs of nitrogen atoms and cytosine bases with silver atoms. The resulting TdT-yielded DNA-AgNCs, which have excellent and unique electro-catalytic performance, can be utilized for TdT activity detection based on the extension role of TdT and the strong interaction between TdT-yielded DNA-AgNCs and graphene oxide (GO) (Hong et al., 2016; Lu et al., 2017). If TdT is pretreated with TdT inhibitors, such as sodium pyrophosphate (PP), activity of TdT will be inhibited, and thus excellent electro-catalytic property of DNA-AgNCs will be diminished. Nay more, the study on electrochemical assay of TdT activity is still unexplored, known to us. Therefore, our sensitive, label-free assay presents a promising and feasible method for bio-electrochemical analysis of critical TdT activity in clinical diagnosis and drug

discovery.

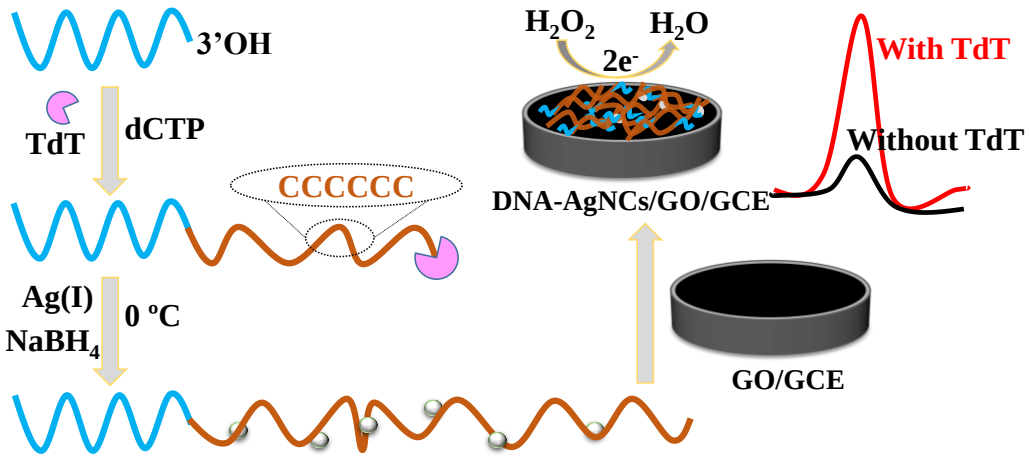

Scheme 1. Schematic diagrams of the synthesis of TdT-generated C-rich DNA nanotail-templated AgNCs and the electrochemical biosensor for probing TdT activity.

In our work, *in situ* grown DNA nanotail-templated AgNCs were synthetized via the nanotails of nitrogen atoms and cytosine bases with silver atoms. And it is also a key factor to achieve the electrochemical detection of TdT activity. Characterization experiments have been done to verify the formation of randomly arrayed C-rich DNA nanotails and DNA-AgNCs, involving fluorescence spectra, DLS and gel electrophoresis experiments. As shown in Figure 1A, grown DNA nanotail-templated AgNCs exhibit an excitation peak centered at 497 nm and an emission peak centered at 562 nm. The obtained results are similar with those obtained by Dickson group (Richards et al., 2008) and Yao group (Xia et al., 2013), and also demonstrate that DNA-AgNCs have been successfully synthesized. Moreover, complete and detailed fluorescence spectra intensity responses of the different samples were displayed in Figure 1B and Figure S1. As we expect, the proposed DNA-AgNCs exhibit strong

fluorescence under the total reaction composition (sample 1), and there is negligible fluorescence for sole composition (sample 2-5, Figure S1A) or deficient composition (sample 6-9, Figure S1B), whose compositions were shown in Figure S1C, indicating an indispensable role on TdT. Moreover, we also investigated the role of $NaBH_4$ and found that a strong fluorescence was displayed with the introduction of $NaBH_4$ (Figure S2). Meanwhile, dynamic light scattering (DLS) data showed that the average hydrodynamic diameter significantly increases to *ca*. 200±15 nm with the formation of DNA-AgNCs (Figure 1C), which is greater than the size of ssDNA before TdT-mediated extension. Additionally, the gel electrophoresis was used to characterize the TdT-generated C-rich DNA nanotails and DNA-AgNCs (Figure 1D). Obviously, the original DNA was elongated under all reaction conditions at lane 6, and in the presence of Ag(I), DNA-AgNCs have a slower electrophoretic migration velocity at lane 7. These results revealed that a random C-rich DNA sequence via TdT polymerization was prepared and was capable of forming DNA-AgNCs successfully.

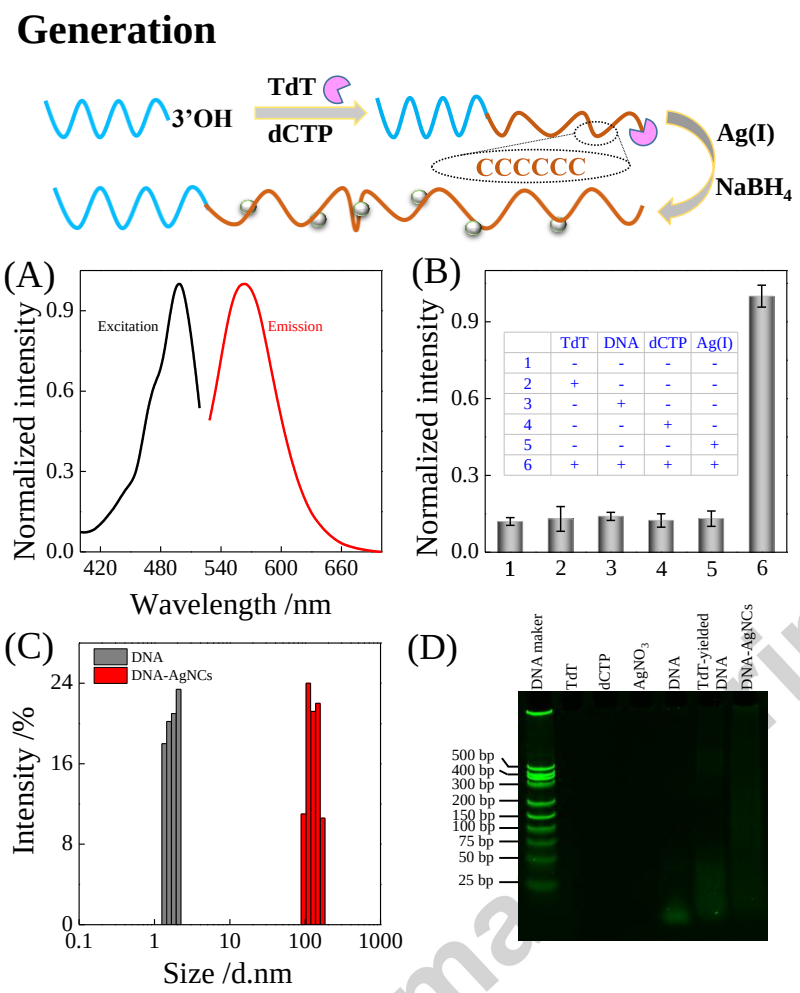

Fig.1. (A) The maximum excitation (497 nm) and emission spectra (562 nm) of the TdT-yielded DNA-AgNCs; (B) Fluorescence emission responses recoded with excitation at 497 nm of the samples and the component of these reaction solutions was shown in the insert diagram: (1) blank solution, (2) sole TdT, (3) sole DNA, (4) sole dCTP, (5) sole $AgNO_3$, (6) all relevant substances involving TdT, DNA, dCTP, and $AgNO_3$; (C) Size distributions of TdT-yielded DNA-AgNCs determined by dynamic light scattering (DLS); (D) PAGE images for characterizing TdT-yielded DNA and DNA-AgNCs. DNA: ssDNA before TdT-mediated extension, TdT-yielded DNA: in-situ TdT-generated C-rich DNA nanotails, DNA-AgNCs: grown DNA nanotail-templated AgNCs.

It is noticeable that a high affinity between ssDNA and GO through π-π stacking interaction has been proved (Zhao et al., 2016). Hence we expected that TdT-generated C-rich DNA nanotail-templated AgNCs, similar to ssDNA, could interact with GO with high affinity, which is one of the prerequisites for electrochemical detection on TdT activity. So, the adsorption of DNA-AgNCs on GO was verified by fluorescence and electrochemical measurements. As noted in Figure 2A, the prepared DNA-AgNCs show a strong fluorescence signal, interestingly, there is a sharp fluorescence decrease at 562 nm after the addition of GO, illustrating a strong interaction occurs between DNA-AgNCs and GO. The obvious fluorescence disappearance can be ascribed to a high quenching efficiency of GO (Zhu et al., 2015; Zhao et al., 2016). Furthermore, we also explored this interaction process with the increasing adsorption time from 0 to 1800 s (Figure S3). After the addition of GO, an outstanding gradual decline on fluorescence was observed within 500 s, but there is almost no change for fluorescence signal after 500 s. These results further support the adsorption interaction of DNA-AgNCs and GO and lay the solid foundation for the following experiments.

Afterwards, we verified the adsorption of DNA-AgNCs on GO by electrochemical measurements and assured the assembly process of the proposed biosensor. As shown in Figure 2B, the cyclic voltammetry signal of $[Fe(CN)_6]^{3-/4-}$ dramatically increases with the electro-deposition of GO (purple) relative to bare GCE (black), indicating effectively accelerating electron transfer by GO modification. The electrochemical signal sharply decreases (red) with the adsorption of DNA-AgNCs efficiently on the

surface of GO/GCE due to the electrostatic repulsion between anionic $[Fe(CN)_6]^{3-/4-}$ and negatively charged phosphate backbone of DNA-AgNCs. However, if the DNA-AgNCs are directly modified on the bare GCE surface (blue), the electrochemical signal has almost unchanged, suggesting the adsorption interaction of GO and DNA-AgNCs. Electrochemical impedance spectroscopy (EIS) was employed to further monitor the assembly process by electron transfer resistance (R_{et}) (Figure 2C). The bare GCE (black) shows a small semicircle, and the succedent GO/GCE (purple) exhibits a lower semicircle due to conductivity of GO. After DNA-AgNCs is coated onto GO/GCE, a sharply increase of R_{et} is observed, while the diameter of semicircular part in the absence of GO (blue) is much smaller than that of DNA-AgNCs/GO/GCE. Subsequently, the prepared sensor was employed for scanning from -0.1 to +0.4 V in 0.1 M PBS solution without H_2O_2. From Figure 2D, a distinctive redox peak at DNA-AgNCs/GO/GCE can be clearly seen, which is attributed to reduction and oxidation of silver of DNA-AgNCs. These results are consistent, further indicative of the adsorption of DNA-AgNCs on GO and the successful assembly of the proposed sensor.

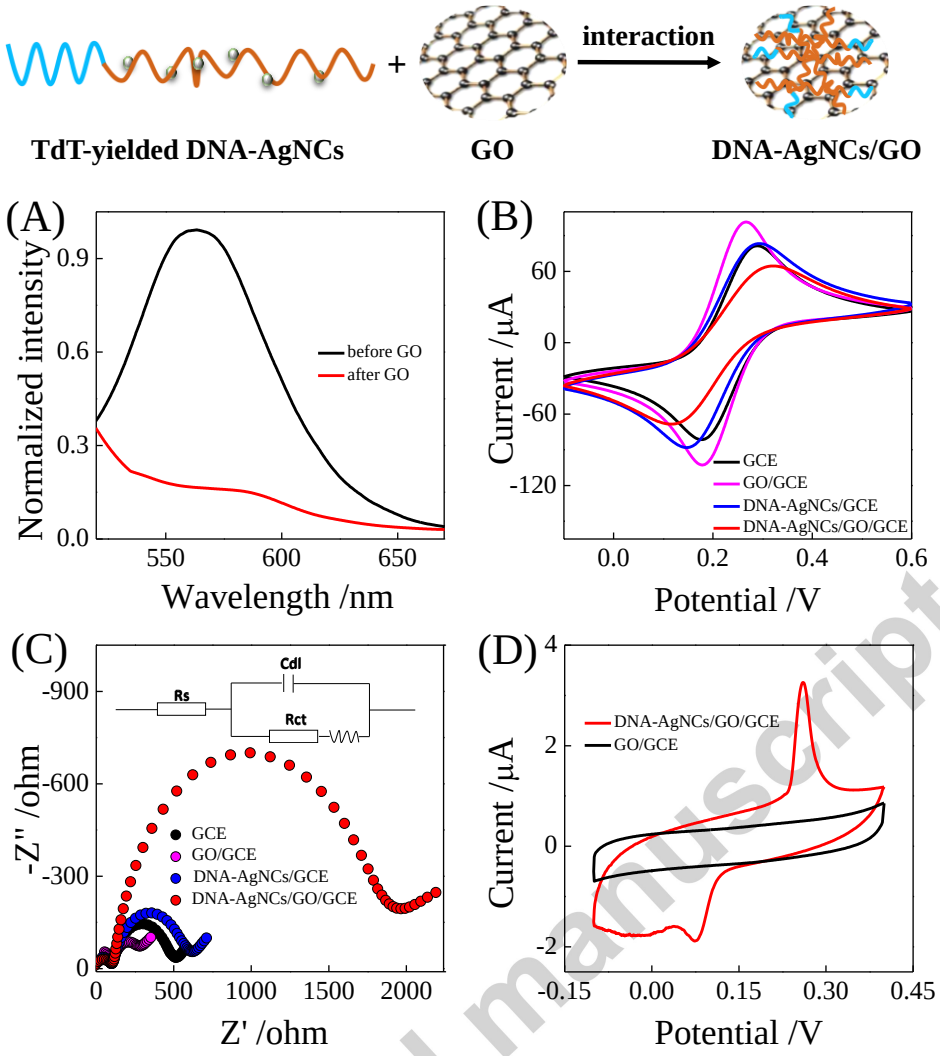

Fig.2. (A) Fluorescence responses of DNA-AgNCs before or after the addition of GO; (B) Cyclic voltammograms of the different modified electrodes from -0.1 to +0.6 V with a scan rate of 50 mV/s and (C) Electrochemical impedance spectra of the different modified electrodes with the frequency range from 10^5 to 10^{-2} Hz at amplitude of 5 mV in 5 mM $[Fe(CN)_6]^{3-/4-}$ containing 0.1 M KCl; (D) Cyclic voltammetry scanning from -0.1 to +0.4 V with a scan rate of 50 mV/s in 0.1 M PBS solution without H_2O_2.

It is intriguing for us to explore the electro-catalytic property of TdT-grown DNA nanotail-templated AgNCs, which is largely scarce. As shown in Figure 3A, both the

bare GCE and GO/GCE show no redox peaks, while an outstanding reduction peak at -0.8 V is observed at DNA-AgNCs/GO/GCE. The absence of TdT or one of other reaction compositions (dCTP, Ag(I) or DNA) also lead to negligible electrochemical signal (Figure 3B and Figure S4), it do foreshadowing for TdT activity detection. We have also tried to directly deposit the DNA-AgNCs on bare electrode (namely DNA-AgNCs/GCE), and no obvious electro-catalytic activity to H_2O_2 reduction was observed (Figure 3C), implying that GO is also important for loading DNA-AgNCs and supporting it to achieve efficient electro-catalytic activity. Furthermore, there is no apparent peak current in the absence of H_2O_2 (Figure 3D), further proving that the current is generated via electro-catalytic activity of DNA-AgNCs toward H_2O_2. In order to further convince the Ag(0) mechanism, the electro-catalysis of Ag(0)/GO/GCE (its fabrication process is displayed in supporting information) toward H_2O_2 was further investigated and the results are shown in Figure S5. The reduction peak potential of H_2O_2 on Ag(0)/GO/GCE (-0.47 V) is more positive than that on DNA-AgNCs/GO/GCE (-0.8 V), implying the higher electro-catalytic activity of electrodeposited Ag(0) than that of adsorbed DNA-AgNCs, which can be ascribed to more Ag(0) loaded on the electrode surface by the electrodeposited Ag(0) process. The corresponding mechanism for electro-catalytic behavior of DNA-AgNCs toward H_2O_2 can be deduced as follows:

$$\mathrm{DNA-Ag(0)NCs - e^- \rightarrow DNA\text{-}Ag(I)NCs} \quad (1)$$

$$\mathrm{DNA-Ag(I)NCs + \tfrac{1}{2} H_2O_2 + e^- \rightarrow DNA\text{-}[Ag(I)\text{-}OH]NCs} \quad (2)$$

$$\mathrm{DNA-[Ag(I)-OH]NCs \rightarrow DNA\text{-}Ag(0)NCs + \tfrac{1}{2} H_2O + \tfrac{1}{4} O_2} \quad (3)$$

where in, DNA-Ag(0)NCs are electrochemically oxidized in step 1 to generate DNA-Ag(I)NCs. Subsequently, DNA-Ag(I)NCs react with H_2O_2 (step 2) to produce DNA-[Ag(I)-OH)]NCs. Finally, in step 3, DNA-[Ag(I)-OH)]NCs are electrochemically reduced to regenerate DNA-Ag(0)NCs and oxidized to generate O_2.

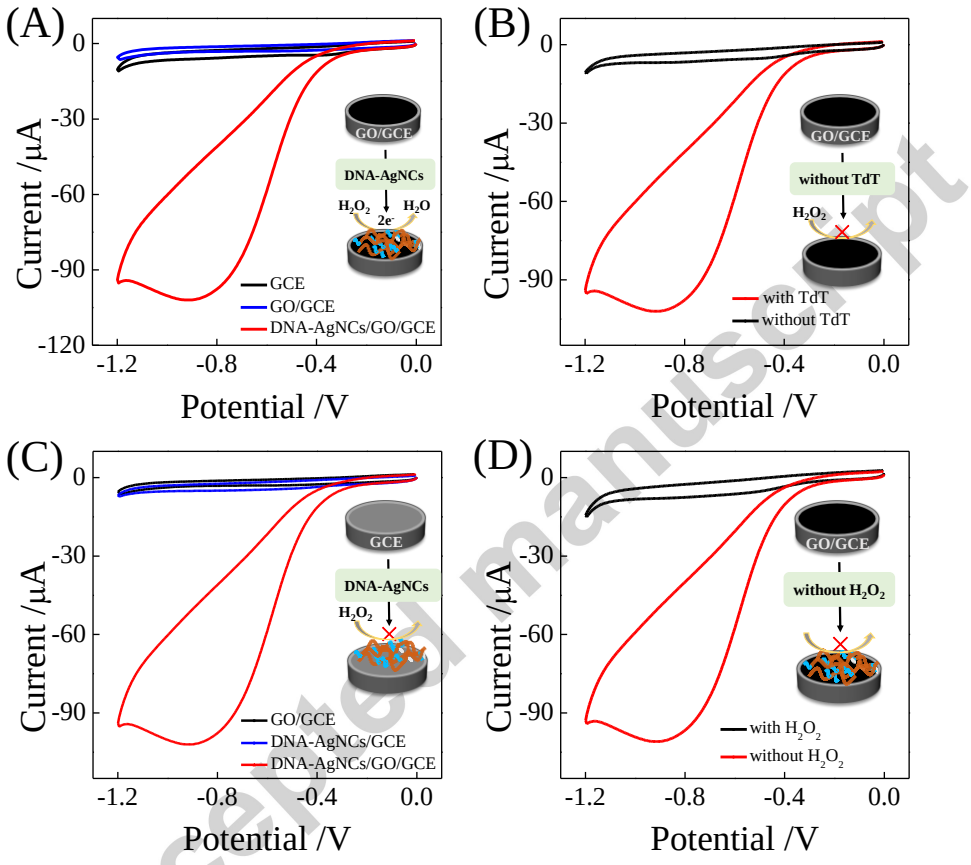

Fig.3. Cyclic voltammetry responses in PBS within the potential range from -1.2 to 0 V with a scanning rate of 50 mV/s: (A) For exploring the unique electro-catalytic property of TdT-yielded DNA-AgNCs in PBS containing 6 mM H_2O_2; (B) In the absence or presence of TdT in PBS containing 6 mM H_2O_2; (C) To prove the interaction between DNA-AgNCs and GO in PBS containing 6 mM H_2O_2; (D) Corresponding to the PBS with or without 6 mM H_2O_2.

3.2. Optimization of experimental conditions

To achieve the high sensitivity of the assay, we optimized the analytical parameters such as the electro-deposition cycles of GO on GCE, TdT-mediated extension time, the absorption time of DNA-AgNCs and GO, pH of detection buffer, which could affect the proposed biosensor response. The GO/GCE after electro-deposition was monitored by cyclic voltammograms with $[Fe(CN)_6]^{3-/4-}$ probe (Figure S6), and the results indicate that the optimal electro-deposition cycle is 5 which offers high current response with the smallest anodic-to-cathodic peak separation (*ΔEp*).

In our strategy, TdT-mediated extension time is related to the synthesis of DNA-AgNCs. Figure S7A exhibits that the response current upon H_2O_2 reduction increases with the increasing TdT-mediated extension time and then approaches a constant value at 1 h. Thus, 1 h of extension time is selected in the following experiments. As noted in Figure S7B, the response current increases with the increasing adsorption time of DNA-AgNCs on GO/GCE, and reaches a plateau from 15 min. A further study was performed to investigate the influence of pH (Figure S7C) and the maximal reduction peak current of H_2O_2 was obtained at pH 7.0. Accordingly, a buffer solution (pH 7.0) is selected as the supporting electrolyte in the experiments.

3.3. Analytical performance test of the proposed biosensor

Under the above-mentioned optimized conditions, we assessed the effect of H_2O_2

concentration on electrochemical signal. As shown in Figure S8A, increasing response currents are observed with the increment of H_2O_2 concentration from 0 to 20 mM. A linear relationship is obtained between increasing current response and H_2O_2 concentrations ranging from 0.001 to 20 mM (Figure S8B), and the detection limit is 0.33 μM (*S/N*=3), which is lower than that of other electrochemical sensor displayed in Table S1. The specificity of the proposed sensor to H_2O_2 was also elucidated by challenging it with several substances (Figure S9), and the proposed sensor shows remarkably high selectivity and good anti-interference to H_2O_2. To testify the potential application of our method in real biological systems, a H_2O_2-trapping test was performed in goat serum (Table S2) or urine (Table S3) samples spiked with different concentrations of H_2O_2. The excellent recoveries indicated good accuracy of the proposed method for complex samples, providing a new insight into H_2O_2-relevant determination in biological fluids.

3.4. Probing TdT activity

The proposed TdT-grown DNA nanotail-templated AgNCs and their electro-catalytic activity were further employed for probing TdT activity. TdT was one of the first DNA polymerases identified in mammalian cells first from thymus and later in bone marrow, nay altered expression levels and activity of TdT have a critical role for cancer development and might worsen the response to anticancer chemotherapy. In the presence of TdT, randomly arrayed C-rich DNA nanotails are obtained by catalyzing the addition of dCTP to the 3'-OH terminus of ssDNA, then used for the synthetic template of AgNCs. The prepared DNA-AgNCs can be readily

loaded on GO-modified electrode and efficiently electro-catalyzed the reduction of H_2O_2, so that TdT activity can be facilely probed by the electrochemical response. Furthermore, the activity of TdT can be quantitatively measured by monitoring DNA-AgNCs generation based on TdT-generated C-rich DNA sequence, which has been proved in Figure 3B and Figure S4 above. Currently, an obvious response current peak of H_2O_2 near -0.8 V appears and the electrochemical response currents of DNA-AgNCs/GO/GCE electrode increase gradually with the increment of concentrations of TdT (Figure 4A). The corresponding calibration curve is shown in Figure 4B, the linear range is from 0.4 to 90 U/mL with a correlation efficiency of 0.9989 and a low limit of detection (LOD) is 0.08 U/mL (*S/N*=3), which is lower than those of most of previously-reported TdT assays (Table S4). Thus, a novel, simple, label-free, and sensitive electrochemical method for TdT activity detection was conducted based on unique electro-catalytic activity of TdT-grown DNA nanotail-templated AgNCs for the first time.

The high selectivity and anti-interference of the assay are crucial for a biosensor to analyze the complex biological samples. As shown in Figure 4C, the specificity of the proposed sensor to TdT was also elucidated by challenging it with several proteins, involving papain, thrombin, lysozyme (LZM) and acetyl cholinesterase (AChE). The electrochemical signal for TdT is much higher than that of other proteins, implying an excellent selectivity. It is probably due to that although these compounds cannot form C-rich DNA nanotails and DNA-AgNCs, causing no signal. Then, the anti-interference is subsequently evaluated and illustrated in Figure 4D, and

negligible change of electrochemical signals were observed, probably resulting from that these compounds are not incapable to interfere TdT activity detection.

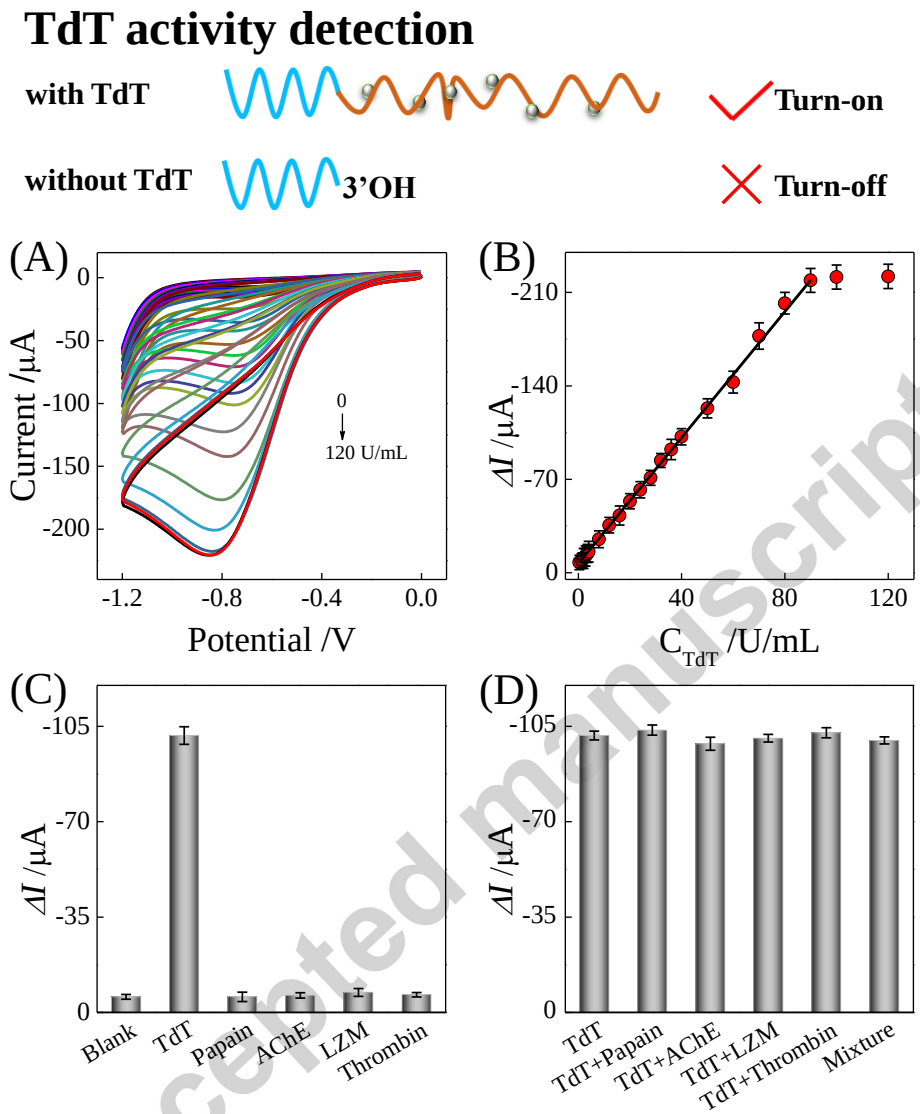

Fig.4. Detection of TdT activity by electrochemical assay at the DNA-AgNCs/GO/GCE in N_2-saturated 0.1 M PBS (pH 7.0) with 6 mM H_2O_2: (A) Cyclic voltammetry in response to different final concentrations of TdT (from top to bottom: 0, 0.4, 1.2, 1.6, 2, 2.4, 2.8, 3.2, 3.6, 4, 8, 12, 16, 20, 24, 28, 32, 36, 40, 50, 60, 70, 80, 90, 100, 120 U/mL); (B) Calibration curve of the proposed TdT sensor; (C) Selectivity and (D) Interference of the prepared TdT sensor, the concentration of all

analysts is 40 U/mL.

Screening of potential small-molecule inhibitors of TdT is of great significance in cancer-targeted drug discovery. To test whether the electrochemical TdT assay can be employed to quantitatively assess TdT inhibitor, $Na_4P_2O_7$ (PP), a potent small molecule inhibitor of the TdT, is used for testing the feasibility of the proposed sensor in inhibitors screening (Peng et al., 2015). As exposed in Figure 5A, the electrochemical indicator declines progressively with growing concentration of PP (Figure 5A) because of the inhibition of TdT activity and thus low level of nanotails extension. Then the IC_{50} value (half maximal inhibitory concentration of the inhibitor) is determined to be 1.9 mM (Figure 5B), which is well dependable with the literature values (Peng et al., 2015). Thus, these results clearly suggest that the TdT-grown DNA nanotail-templated AgNCs-based sensor assay has a considerable potential to qualitatively screen TdT inhibitors.

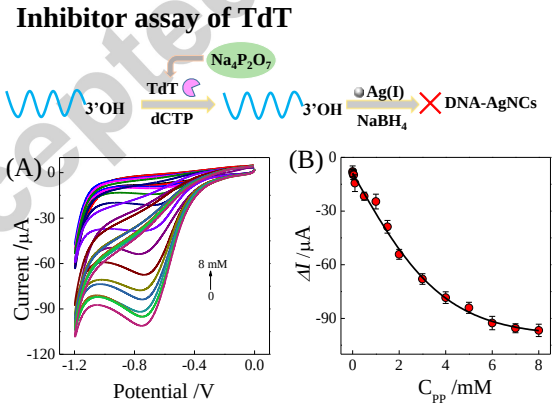

Fig.5. Detection of TdT inhibition by the electrochemical assay at DNA-AgNCs/GO/GCE in N_2-saturated 0.1 M PBS (pH 7.0) with 6 mM H_2O_2: (A) Various final concentrations of $Na_4P_2O_7$ (PP) were used for investigation of TdT inhibition. From bottom to top: 0, 0.01, 0.02, 0.05, 0.1, 0.5, 1, 1.5, 2, 3, 4, 5, 6, 7 and

8 mM; (B) Electrochemical signal as a function of the concentration of $Na_4P_2O_7$ (PP).

3.5. Repeatability, stability and real application of the proposed sensor

The repeatability and stability are essential evaluation index for excellent TdT-based electrochemical biosensor, so eight DNA-AgNCs modified electrodes were investigated at the same condition by comparing their cyclic voltammetry responses. As shown in Figure S10A, the negligible difference on the current response was displayed, presenting an excellent repeatability. Furthermore, the storage stability of the biosensor was investigated by monitoring its response to 6 mM H_2O_2 (Figure S10B) by successive assays. After a month, the proposed sensor remains stable and the response current is approximately 82.8% of the original current. These results indicate that the electrochemical sensor is a potent platform for the sensitive detection of TdT activity.

The proposed sensor presents a novel and efficient mechanism for electrochemical detection of TdT activity. To testify the potential application of our method in real biological systems, a TdT-trapping test was performed in goat serum or urine samples spiked with different concentrations of TdT. The recoveries are between 95.6% and 105.4% in goat serum (Table S5), or between 98.3% and 103.7% in urine (Table S6), indicating good accuracy of the proposed method for complex samples, which clearly provided the potentiality of this assay in real biological samples.

4. Conclusions

Herein, the randomly arrayed C-rich DNA sequence prepared by TdT

polymerization could serve as the template of AgNCs with unique electro-catalytic property. By exploiting the interaction between TdT-generated C-rich DNA nanotail-templated AgNCs and GO, we firstly developed a novel, label-free detection strategy by *in situ* grown DNA nanotail-templated silver nanoclusters enabling electrochemical sensing of TdT activity. These findings might have a potential impact on multifarious aspects: (1) TdT combined with dCTP provides a new method to prepare a C-rich DNA-nanotails, which is employed for the synthetic template of AgNCs; (2) a TdT-generated randomly arrayed C-rich DNA nanotail-templated AgNCs act as a signal producer by the adsorption interaction with GO; (3) the electrochemical sensing of TdT activity and its inhibitor is seldom. Ultimately, our electrochemical assay displays excellent sensitivity and selectivity, and presents a promising and feasible method for TdT activity detection in clinical diagnosis and drug discovery.

Acknowledgements

Financial support from the National Natural Science Foundation of China (41576098, 81273130 and 21605089), the Open Subject of State Key Laboratory of Chemo/Biosensing and Chemometrics (2016001), Project of Academic Research Foundation of Ningbo University (XYL17002), the Ningbo Municipal Natural Science Foundation (2016A610052), and the Science and Technology Department of Zhejiang Province of China (2016C33176, 2016R405068) are gratefully acknowledged. This work was also sponsored by K.C. Wong Magna Fund in Ningbo

University.

References

Benedict, C.L., Gilfillan, S., Thai, T.H., Kearney, J.F., 2000. Immunol. Rev. 175, 150-157.

Benedict, C.L., Kearney, J.F., 1999. Immunity 10, 607-617.

Bollum, F.J., 1960. J. Biol. Chem. 235, 2399-2403.

Bollum, F.J., 1964. Science 144, 560.

Elghanian, R., Storhoff, J.J., Mucic, R.C., Lesinger, R.L., Mirkin, C.A., 1997. Science 277, 1078-1081.

Feng, J.J., Zhuo, C.X., Ma, X.J., Li, S.Q., Zhang, Y.D., 2016. Analyst 141, 4481-4487.

Goldschneider, I., Gregoire, K.E., Barton, R.W., Bollum, F.J., 1977. Proc. Natl. Acad. Sci. U. S. A. 74, 734-738.

Gopalakrishnan, A.M., Kumar, N., 2003. Nature 421, 431-435.

Greaves, M., Paxton, A., Janossy, G., Pain, C., Johnson, S., Lister, T.A., 1980. Leuk. Res. 4, 1-14.

Hoffbrand, A.V., Ganeshaguru, K., Janossy, G., Greaves, M.F., Catovsky, D., Woodruff, R.K., 1977. Lancet, 310, 520-523.

Hong, C., Baek, A., Hah, S.S., Jung, W., Kim, D., 2016. Anal. Chem. 88, 2999-3003.

Javani, S., Lorca, R., Latorre, A., Flors, C., Cortajarena, A.L., Somoza, Á., 2016. ACS Appl. Mater. Interfaces 8, 10147-10154.

Hu, Y.F., Shen, Q.P., Li, W., Liu, Z.L., Nie, Z., Yao, S.Z., 2015. Biosens. Bioelectron. 63, 331-338.

Jin, R.C., Zeng, C.J., Zhou, M., Chen, Y.X., 2016. Chem. Rev. 116, 10346-10413.

Jin, S., Wang, S.X., Xiong, L., Zhou, M., Chen, S., Du, W.J., Xia, A.D., Pei, Y., Zhu, M.Z., 2016. Chem. Mater. 28, 7905-7911.

Krayevsky, A.A., Victorova, L.S., Arzumanov, A.A., Jasko, M.V., 2000. Pharmacol. Ther. 85, 165-173.

Kung, P.C., Long, J.C., McCaffrey, R.P., Ratliff, R.L., Harrison, T.A., Baltimore, D., 1978. Am. J. Med. 64, 788-794.

Kung, P., Gottlieb, P., Baltimore, D., 1976. J. Biol. Chem. 251, 2399-2404.

Labib, M., Sargent, E.H., Kelley, S.O., 2016. Chem. Rev. 116, 9001-9090.

Liu, S.F., Wei, W.J., Sun, X.Y., Wang, L., 2016. Biosens. Bioelectron. 83, 33-38.

Liu, X.R., Hu, R.X., Gao, Z.D., Shao, N., 2015. Langmuir 31, 5859-5867.

Liu, Z.L., Li, W., Nie, Z., Peng, F.F., Huang, Y., Yao, S.Z., 2014. Chem. Commun. 50, 6875-6878.

Lu, C., Liu, Y.B., Ying, Y.B., Liu, J.W., 2017. Langmuir, 33, 630-637.

Mahshid, S.S., Camiré, S., Ricci, F., Bélisle, A.V., 2015. J. Am. Chem. Soc. 137, 15596-15599.

Peng, F.F., Liu, Z.L., Li, W., Huang, Y., Nie, Z., Yao, S.Z., 2015. Anal. Methods. 7, 4355-4361.

Richards, C.I., Choi, S., Hsiang, J.C., Antoku, Y., Vosch, T., Bongiorno, A., Tzeng, Y.L., Dickson, R.M., 2008. J. Am. Chem. Soc. 130, 5038-5039.

Shen, Q.M., Han, L., Fan, G.C., Zhang, J.R., Jiang, L.P., Zhu, J.J., 2015. Anal. Chem. 87, 4949-4956.

Singh, M., Bhardiya, S.R., Kashyap, H., Verma, F., Rai, V.K., Tiwari, I., 2016. RSC Adv. 6, 104868-104874.

Venditti, A., Del Poeta, G., Buccisano, F., Tamburini, A., Aronica, G., Bruno, A., Cox, M.C., Maffei, L., Simone, M.D., Papa, G., Amadori, S., 1997. Blood 89, 345-346.

Wang, Z.G., Liu, Q., Li, N., Ding, B.Q., 2016. Chem. Mater. 28, 8834-8841.

Wang, P.J., Wan, Y., Deng, S.Y., Yang, S.L., Su, Y., Fan, C.H., Aldalbahi, A., Zuo, X.L., 2016. Biosens. Bioelectron. 86, 536-541.

William, W.S., Hummers, J.R., Richard, E.O., 1958. J. Am. Chem. Soc. 80, 1339-1339.

Xia, Y.L., Li, W.H., Wang, M., Nie, Z., Deng, C.Y., Yao, S.Z., 2013. Talanta 107, 55-60.

Yang, C.Y., Shi, K., Dou, B.T., Xiang, Y., Chai, Y.Q., Yuan, R., 2015. ACS Appl. Mater. Interfaces 7, 1188-1193.

Yuan, Y.J., Li, W.H., Liu, Z.L., Nie, Z., Huang, Y., Yao, S.Z., 2014. Biosens. Bioelectron. 61, 321-327.

Zhang, M.W., Hou, C.Y., Halder, A., Wang, H.Z., Chi, Q.J., 2017. Mater. Chem. Front. 1, 37-60.

Zhao, M., Chen, A.Y., Huang, D., Zhuo, Y., Chai, Y.Q., Yuan, R., 2016. Anal. Chem. 88, 11527-11532.

Zhao, Q.C., Zhou, Y.Y., Li, Y.Y., Gu, W., Zhang, Q., Liu, J., 2016. Anal. Chem. 88, 1892-1899.

Zhu, Y.Y., Cai, Y.L., Xu, L.G., Zheng, L.X., Wang, L.M., Qi, B., Xu, C.L., 2015. ACS

Appl. Mater. Interfaces 7, 7492-7496.

Highlights

- Randomly arrayed C-rich DNA nanotails were presented via catalysis of terminal deoxynucleotidyl transferase (TdT).
- TdT-generated C-rich DNA sequence was employed for the synthetic template of silver nanoclusters (AgNCs).
- In situ grown DNA nanotail-templated AgNCs adsorbed on GO-modified electrode possessed high electro-catalytic activity.
- The proposed label-free electrochemical biosensor was used for TdT activity detection and inhibitor screening.
- The developed TdT electrochemical sensing platform exhibits excellent sensitivity, selectivity and anti-interference.